

Robust Stereo Matching Using Improved ZNCC Combined SAD-LBP

Jieqiong Chen
Fuzhou University
Fuzhou Fujian, China
linfzu7@163.com

Yousheng Xia
Fuzhou University
Fuzhou Fujian, China
ysxia@fzu.edu.cn

ABSTRACT

Stereo matching aims to obtain depth information of scene from captured images, which becomes an active research topic in the field of computer vision. Most stereo matching cost algorithms are based on a common assumption, which is the intensity or color value of corresponding pixels are same. However, in real-world applications, the colors of the objects observed in the recorded image data are affected by radiometric variations. In this paper, using a novel similarity measure we propose a robust stereo matching method, which has robust performance to noise, illumination condition changes, and exposure changes between left and right images. The proposed stereo matching cost combines improved zero mean normalized cross-correlation (ZNCC) model and the absolute difference of local binary pattern (LBP) of windows to get both the color and texture similarity of windows to be matched. Based on Middlebury data set, we verify the effectiveness of the proposed algorithm. Computed results show that the proposed algorithm is more robust to illumination changes and noise than related stereo matching algorithms.

CCS Concepts

Computing methodologies→Matching

Keywords

Stereo matching; Radiometric variation; Noise.

1. INTRODUCTION

Stereo matching aims to restore the depth information of scene, which lost in procedure of projecting the three-dimensional real scene into the two-dimensional image. To achieve this purpose, stereo matching finds the correct correspondence from multi-view images. The majority of state-of-the-art algorithms are based on a common assumption called color consistency, in which the corresponding pixels should have same intensities or color values. However, in real-world applications, due to the variations in imaging condition such as illumination, camera characteristic and lighting geometry, color values of corresponding pixels no

longer equal to each other. The color of the object observed in

the recorded image data usually cannot fully describe the properties of the object itself, but also depending on the lighting conditions in which the object is observed. In addition, even under the same lighting condition, the color of objects may be different depending on camera characteristics [1]. Human visual system can automatically adjust the chromatic aberration of the image being seen and maintain its high fidelity. However, it is not easy for computer algorithms to recognize imaging conditions and mitigate its effects.

In this paper, we present a new similarity measure which shows robust to illumination condition changes, exposure changes and noise. It could be useful in global radiometric changes caused by different imaging condition, such as illuminant color, camera characteristic or noise, and also be useful in local radiometric changes caused by different lighting geometry and so on. The proposed similarity measure combined both the color feature and the texture feature of window centered on pixels to be matched. We use Middlebury data set [2] to test and verify the performance of proposed algorithm.

2. RELATED WORKS

Hirschmüller et.al carried out a paper [3] which summarized commonly used matching cost methods that handle radiometric differences and gave an evaluation on them. Normalized cross-correlation(NCC) [4] is a typical window-based matching cost for contrast-varying images. A major drawback of NCC is that it suffers from the fatten effect near object boundaries. Zero-normalized cross-correlation, also known as ZNCC, as its name suggests, is the zero-mean version of NCC. ZNCC is only parametric cost that can compensate for differences in both gain and offset within the correlation windows. Census [5] is a non-parametric matching costs only relies on the local order of pixel values. Census is not only fast and efficient but also robust to radiometric changes, and Census is more robust near object boundaries. These advantages mentioned above make Census a relatively widely used method in state-of-the-art papers.

Mutual information (MI) first has been introduced into stereo matching as a similarity measure [6]. Kim et al. [7] proposed a pixel-based matching cost without using matching windows based on mutual information, and used it in the graph cuts. Hirschmüller et al. [8] improved Kim's work by using a hierarchical mutual information (HMI), which speeded up the calculation of pixel-wise MI, and it is as accurate as an iterative calculation.

Based on the framework of ZNCC, Heo et al. [9] proposed an edge-preserving similarity measure named Adaptive Normalized Cross-Correlation, which is a robust and accurate method for image pairs with radiometric variations. KHAN et al. [10] proposed a similarity metric named Intensity Guided Cost

Permission to make digital or hard copies of all or part of this work for personal or classroom use is granted without fee provided that copies are not made or distributed for profit or commercial advantage and that copies bear this notice and the full citation on the first page. Copyrights for components of this work owned by others than ACM must be honored. Abstracting with credit is permitted. To copy otherwise, or republish, to post on servers or to redistribute to lists, requires prior specific permission and/or a fee. Request permissions from Permissions@acm.org.

ICMIP 2020, January 10 - 12, 2020, Nanjing, China

© 2020 Association for Computing Machinery.

ACM ISBN 978-1-4503-7664-8/20/01...\$15.00

<https://doi.org/10.1145/3381271.3381295>

Metric (IGCM), which built a weighted NCC and used guided filtering to implicitly compute the weights. Although both using the same framework, the calculation speed of IGCM has been greatly improved compared to ANCC and NCC. Yang et al. [11] proposed a similarity measure which is invariant to global and local affine illumination changes, and its computational complexity is relatively low.

3. RADIOMETRIC ROBUST STEREO CORRESPONDENCE

3.1 Proposed Similarity Measure

Let us define I_L and I_R as the left and right image of stereo image pairs, respectively. Let p be a pixel, $I_L(p)$ denote the intensity value in the left image at pixel p and $I_R(p + f_p)$ is the intensity value in the right image at pixel $p + f_p$. f_p is a variable representing possible disparity for pixel p . Zero Mean Normalized Cross-Correlation (ZNCC) can be represented as following:

$$ZNCC(f_p) = \frac{\sum_{t_L \in w_L(p), t_R \in w_R(p+f_p)} [I_L(t_L) - \bar{I}_L(p)] \times [I_R(t_R) - \bar{I}_R(p+f_p)]}{\sqrt{\sum_{t_L \in w_L(p)} |I_L(t_L) - \bar{I}_L(p)|^2 \times \sum_{t_R \in w_R(p+f_p)} |I_R(t_R) - \bar{I}_R(p+f_p)|^2}} \quad (1)$$

where $w_L(p)$ is a square window centered at pixel p in I_L with window size m , identically $w_R(p + f_p)$ is a square window centered at pixel $p + f_p$ in I_L with same window size. $\bar{I}_L(p)$ and $\bar{I}_R(p)$ are the mean intensity values of pixels in $w_L(p)$ and $w_R(p + f_p)$. The similarity defined by ZNCC ranges from -1 to +1

The original ZNCC model still has some drawbacks. There is blur around the objects' boundaries in the depth map of ZNCC, which is called fatten effect, since all pixels in the windows contribute equally to the similarity in the framework of ZNCC. We desire center pixel contributing most and pixels closer to center pixel contributing more, therefore the weighted ZNCC model is needed. The weighted ZNCC model can circumvent this fatten effect and obtain a more accurate disparity map. On the basis of the original ZNCC model, we propose an improved ZNCC model as follows:

$$WZNCC(f_p) = \frac{\sum_{t_L \in w_L(p), t_R \in w_R(p+f_p)} W_L(t_L) J_L(t_L) \times W_R(t_R) J_R(t_R)}{\sqrt{\sum_{t_L \in w_L(p)} |W_L(t_L) J_L(t_L)|^2 \times \sum_{t_R \in w_R(p+f_p)} |W_R(t_R) J_R(t_R)|^2}} \quad (2)$$

In the selection of the weights $W_v(\cdot)$, $v \in [L, R]$, in order to maintain the speed of the calculation, we chose the isotropic Gaussian weight. For each point in the window, it only depends on the size of the window and the position of this point relative to the center point, closer to the center point bigger the weight is. So, for a window with fixed size, the weights can be obtained in advance, without having to recalculate the weights once for each window. The weights are computed as follows:

$$W_L(t_L) = \exp\left(-\frac{\|p - t_L\|^2}{2\sigma_d^2}\right), W_R(t_R) = \exp\left(-\frac{\|p + f_p - t_R\|^2}{2\sigma_d^2}\right) \quad (3)$$

Different from other weighted ZNCC, which compares the intensity values with the mean value of pixels in the left and right windows, the proposed WZNCC utilize the $W_L(t_L) J_L(t_L)$ and

$W_R(t_R) J_R(t_R)$ extracted from left and right windows respectively to get the similarity, where $J_L(t_L)$ and $J_R(t_R)$ is given by:

$$J_L(t_L) = I_L(t_L) - \bar{I}_L(p), J_R(t_R) = I_R(t_R) - \bar{I}_R(p + f_p) \quad (4)$$

In the framework of ZNCC, the mean intensity values of pixels in the window \bar{I} is computed for the similarity. We construct \bar{I} in equation (5), which is all the pixels in the window multiplied by the kernel weights of guided filter [12] and sum them all. Using \bar{I} in ZNCC model can compensate for differences in both gain and offset within windows better than using \bar{I} directly. Next, we take the calculation in left image as an example. The calculation for right image is exactly the same

$$\bar{I}_L(p) = \sum_{t \in w(p)} W_L^{(G)}(t) I_L(p) \quad (5)$$

where the kernel weight $W_L^{(G)}$ is defined as following:

$$W_L^{(G)}(t) = \frac{1}{|\omega|} \sum_{t \in w(p)} \left(1 + \frac{(G_L(p) - \mu(p))(G_L(t) - \mu(p))}{\sigma^2(p) + \varepsilon}\right) \quad (6)$$

G_L is a guidance image, while I_L is the filtering input image. We use the reference image I_L itself as the guidance image. $\mu(p)$ and $\sigma^2(p)$ are the mean and variance of G_L in local window centered on p . $|\omega|$ is the number of pixels in window $w(p)$. Equation (5) can be equivalently rewritten as (7), for easier calculation, basing on the article of guided filtering [12].

$$\bar{I}_L(p) = \bar{a}_p G_L(p) + \bar{b}_p \quad (7)$$

where linear coefficients \bar{a}_p and \bar{b}_p can be represented as follows:

$$\bar{a}_p = \frac{1}{|\omega|} \sum_{t \in w(p)} a_t, \bar{b}_p = \frac{1}{|\omega|} \sum_{t \in w(p)} b_t \quad (8)$$

where the solution of a_t and b_t is given by:

$$a_t = \frac{\frac{1}{|\omega|} \sum_{t \in w(p)} G_L(t) I_L(t) - \mu(t) \bar{I}_L(t)}{\sigma^2(p) + \varepsilon}, b_t = \bar{I}_L(t) - a_t \mu(t) \quad (9)$$

In the framework of proposed WZNCC, to measure the similarity of two points in the left and right images, we build a window centered on them and using WZNCC model to evaluate their color similarity. But we hope to measure the similarity of these two points more comprehensively, so we also evaluate the texture similarity of them, since the texture features of the objects do not change with the radiometric variation. We build a model based on the local binary pattern (LBP) [13] to measure the texture similarity between the windows in left and right images.

We define a 3×3 size block B_i centered on point p_i , and each point in the block corresponds to its intensity. From the bottom left point, the points other than the center point p_i in the block B_i are compared with the center point p_i in counterclockwise order. If the intensity value of this point is bigger than intensity of point p_i , it is counted as 1; if otherwise, it is counted as 0. Therefore this 3×3 size block is transformed into an 8-bit array consisting of only 0 and 1. An 8-bit binary array can be converted to a decimal integer. We replace the intensity value of point p_i with this newly obtained integer and normalize it, we record it as $T(p_i)$. By performing such an operation on each point on the graph, we can obtain a texture map that does not affected by factors such as ambient light.

$$T(p_i) = \sum_{j=0}^7 S(p_j - p_i) 2^{(8-j)} / 255, S(x) = \begin{cases} 1 & x > 0 \\ 0 & x \leq 0 \end{cases} \quad (10)$$

Therefore, in the left image, we can take a square window centered on point p with a window size m . The number of the pixels in the window is $m \times m$, and it is recorded as M . Each pixel

in the window corresponds to an integer obtained by equation (10), and it is denoted as $T_L(t_i)$, $i \in [1, M]$, and the set of all $T_L(t_i)$ in the window is denoted as $T_L(p)$. For the right picture, repeat the operation above, and the obtained set of points denoted as $T_R(p + f_p)$.

$$T_L(p) = (T_L(t_1), \dots, T_L(t_M)), M = m \times m \quad (11)$$

$$T_R(p + f_p) = (T_R(t_1), \dots, T_R(t_M)), M = m \times m \quad (12)$$

The set $T_L(p)$ represents the texture of the window centered on point p in the left image, and similarly, $T_R(p + f_p)$ represents the texture of the window centered on point $p + f_p$ in the right image. The similarity between $T_L(p)$ and $T_R(p + f_p)$ is defined by its sum of absolute difference as follows:

$$AT(f_p) = \sum_{i=1}^M |T_L(t_i) - T_R(t_i)| \quad (13)$$

where $T_L(t_i) \in w_L(p)$ and $T_R(t_i) \in w_R(p + f_p)$. Combining equation (2) and (13), we define the data cost $D_p(f_p)$ as follows:

$$D_p(f_p) = \alpha(1 - WZNCC(f_p)) + \beta(AT(f_p)) \quad (14)$$

where α and β are weighting factor between $WZNCC(f_p)$ and $AT(f_p)$. The proposed algorithm flow is as shown in Algorithm 1.

Algorithm 1 Computation of data cost for the proposed algorithm.

Input:

Stereo images I_L and I_R , guided images G_L and G_R ;

Set window size as m , regularization parameter ε , kernel parameter σ_d , weight parameter α and β ;

1: Obtain \bar{a}_L , \bar{b}_L , \bar{a}_R , \bar{b}_R with the algorithm proposed in [12];

2: Construct $\tilde{I}_L(\cdot)$, $\tilde{I}_R(\cdot)$ using (7);

3: Construct $J_L(\cdot)$, $J_R(\cdot)$ using (4);

4: Construct isotropic Gaussian weight $W_L(\cdot)$, $W_R(\cdot)$ using (3);

5: Convert I_L , I_R to LBP texture map using (10);

6: For each pixel p in I_L , disparity f_p

1) Construct window $w_L(p)$ in I_L and $w_R(p + f_p)$ in I_R ;

2) Obtain $WZNCC(f_p)$ using (2);

3) Obtain $AT(f_p)$ using (13);

4) Compute data cost

$$D_p(f_p) = \alpha(1 - WZNCC(f_p)) + \beta(AT(f_p));$$

End;

Output:

$D_p(f_p)$: Data cost for disparity f_p at pixels p in I_L .

3.2 Comparison with Related Work

As mentioned above, ANCC used ZNCC model with bilateral filtering weights as the framework, and constructed the log-chromaticity color basing on the color generation model to eliminate the influence of the radiometric changes. The log-chromaticity color is relatively robust to radiometric changes, but it is sensitive to noise. In ANCC, the similarity of windows is calculated six times from six channels consisting of RGB and log-chromaticity RGB, that makes the calculation speed slow. IGCM is an improvement of ANCC algorithm, which followed its idea of the log-chromaticity color. Different from ANCC, IGCM combined the guided filtering on the weighted NCC model to

convert the similarity measure from window-based to pixel-wise to increase the calculation speed.

The proposed algorithm measures the color and texture similarity of windows. Similar to ANCC, the proposed algorithm also used the weighted ZNCC model when measured the color similarity of windows. However, in order to maintain the calculation speed, we only considered the intensity value, therefore the similarity calculation only needs to be done once, and it is more robust to noise. In order to maintain accuracy and speed, we introduced guided filtering into the weighted ZNCC model, but different from the derivation process of IGCM, our algorithm is still window-based. In addition, we also used the absolute difference of local binary pattern of windows to measure the texture similarity between them.

4. EXPERIMENTAL RESULT

The proposed algorithm was implemented using Matlab 2016a. In our experiments, the parameter settings of the proposed algorithm were as follows: $\varepsilon = 0.01$, $\sigma_d = 7$, $\alpha = 15$, $\beta = 0.5$. The window size m was taken as 15. We select weights of both the intensity and texture similarity terms by selecting a range based on their values and test a set of different parameters within that range.

We used the middlebury test data sets to evaluate the proposed algorithm. A total of 4 data sets (including cloth4, dolls, moebius and rocks1) were used for our testing. Each of these data sets contains three different illuminations (indexed as illum1, illum2 and illum3) and three different exposures (indexed as exp0, exp1, exp2). When we evaluated the illumination changes, the exposure was set to 'exp1'; and when we evaluated the exposure changes, the illumination is set to 'illum2'. It is worth noting that when we designed the experiment, we avoided the same combination of illumination and exposure for left and right image, such as illum1/2 (left/right) and illum2/1(left/right). This is because for the same combination of illumination and exposure, the property of it remains unchanged.

In the experiment part, in order to evaluate our similarity measure algorithm, we compared it with similarity measure including NCC [4], Census [5], ANCC [9], pixel-based ANCC [14], IGCM [10] on phase calculating matching cost. And then for all these similarity measures we used local tree-filter [15] to aggregate the matching cost obtained. Finally, Winner-Take-All disparity selection scheme was applied to the cost aggregated using local tree-filter to obtain the disparity map. And then we compared the proposed method with MC-CNN [16] to evaluate the results of only the similarity measure with WTA. We calculated and compared the error rate in unoccluded areas.

4.1 Light Source Changes

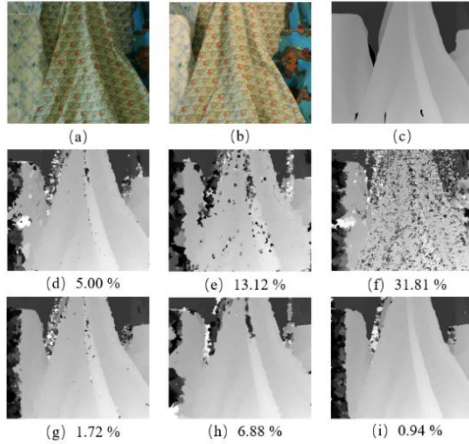


Figure 1 Disparity map obtained by test algorithms on stereo images ‘Cloth4’ with illumination changes. (a) Left image (with illum1/exp2). (b) Right image (with illum2/exp2). (c) The ground truth disparity map. (d) Census. (e) IGCM. (f) Pixel-based ANCC. (g) ANCC. (h) NCC. (i) The proposed algorithm

In order to evaluate the difference of disparity map under different illumination, we fixed the index of exposure to 1, and varied the index of illumination from 1 to 3. Fig. 1 shows one of the experiment results on the ‘Cloth4’ data set with illumination combination illum1/exp1 and illum2/exp1. Fig. 1d-1i shows disparity maps obtained by test stereo algorithms and the subscript shows its error rate of unoccluded areas. The configuration of Fig. 2 and Fig. 1 is the same. Fig. 2 shows one of the experiment results on the ‘Dolls’ data set with illumination combination illum2/exp1 and illum3/exp1.

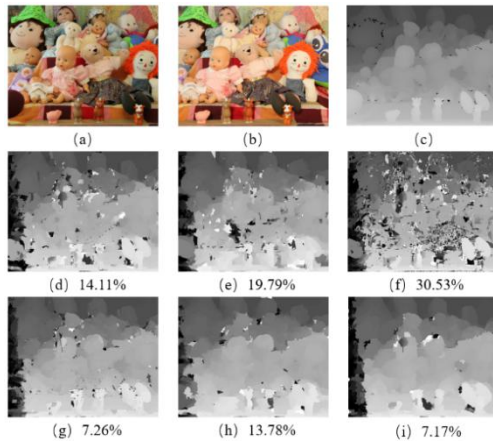


Figure 2. Disparity map obtained by test algorithms on stereo images ‘Dolls’ with illumination changes. (a) Left image (with illum2/exp2). (b) Right image (with illum3/exp2). (c) The ground truth disparity map. (d) Census. (e) IGCM. (f) Pixel-based ANCC. (g) ANCC. (h) NCC. (i) The proposed algorithm.

Different illumination means images captured under different light source, which would cause local radiometric changes. It has always been a difficult problem to find corresponding pixels from stereo image pairs with local radiometric changes. We can find pixels-based ANCC is sensitive to local radiometric changes, since it partially uses derivative of intensity. IGCM has larger error than ANCC when using tree-filter as cost aggregation. ANCC has a good performance in the local radiometric changes, but its

calculation speed is extremely slow. And ANCC does not perform well in the occluded areas. As NCC only assumes a global radiometric change, so in the situation of local radiometric changes it performs in general. Census performs well in slight local illumination changes, for extreme illumination changes its accuracy is declining. The proposed method performed well in the case of local radiometric changes, and as a window-based algorithm it needs to calculate once per window, and it performed well in the occluded areas.

4.2 Camera Exposure Changes

In order to evaluate the difference of disparity map under different exposure, similar to above section, we fixed the index of illumination to 2, and varied the index of exposure from 0 to 2. Fig. 3 shows one of the experimental results on ‘Rocks1’ data set with exposure combination illum2/exp0 and illum2/exp2. Fig. 3d-3i shows disparity maps obtained by test stereo algorithms and the subscript shows the error rate of unoccluded areas. The configuration of Fig. 4 and Fig. 3 is the same. Fig. 4 shows one of the experiment results on the ‘Moebius’ data set with exposure combination illum2/exp0 and illum2/exp2.

Different exposure means images captured under camera exposure condition, which would cause global radiometric changes. Overexposed (exp2) would make images captured extremely bright, and underexposure (exp0) would make images captured extremely dark. We can find NCC does not perform well in the situation of extreme exposure changes, and the boundaries of the objects in the disparity map is severely blurred. Pixels-based ANCC has better performance around the boundaries of the objects, but it performs bad on more textured image in the situation of extreme exposure changes. IGCM using tree-filter as cost aggregation also performs not well and it suffer from blurred around the boundaries. ANCC has a good performance in the global radiometric changes, but its calculation speed is extremely slow. Census performs well in the situation of extreme exposure changes.

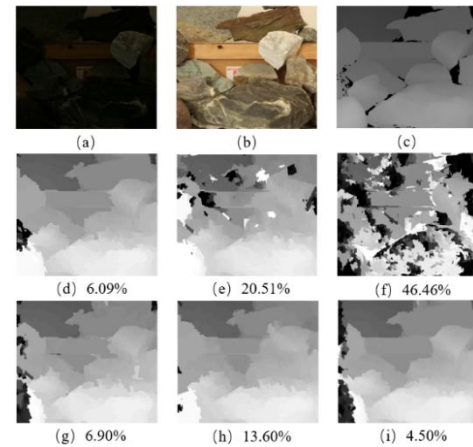


Figure 3. Disparity map obtained by test algorithms on stereo images ‘Rocks1’ with exposure changes. (a) Left image (with illum2/exp0). (b) Right image (with illum2/exp2). (c) The ground truth disparity map. (d) Census. (e) IGCM. (f) Pixel-based ANCC. (g) ANCC. (h) NCC. (i) The proposed algorithm.

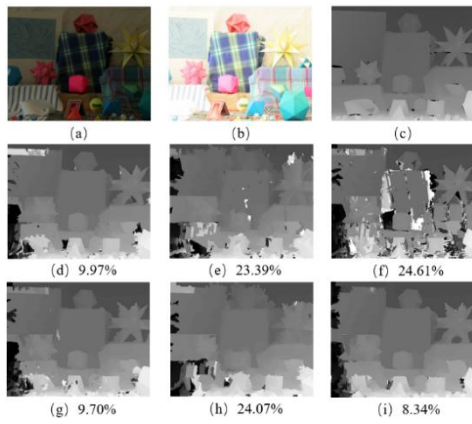


Figure 4. Disparity map obtained by test algorithms on stereo images ‘Moebius’ with exposure changes. (a) Left image (with illum2/exp0). (b) Right image (with illum2/exp2). (c) The ground truth disparity map. (d) Census. (e) IGCM. (f) Pixel-based ANCC. (g) ANCC. (h) NCC. (i) The proposed algorithm.

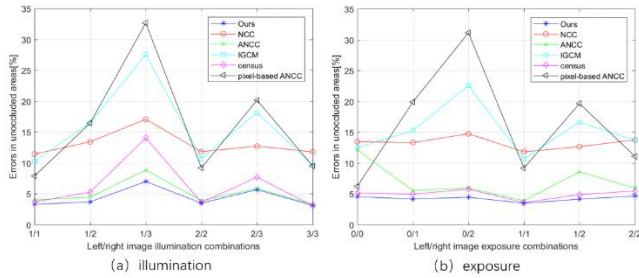


Figure 5. The average percentages of errors in unoccluded areas of test algorithms under different illumination (a)/ exposure (b) combinations on 4 data sets.

The proposed method performs well in the case of global radiometric changes, and it gives reliable disparities in both the occlusion areas and the boundaries of the objects. The average percentages of errors in unoccluded areas of test algorithms under different illumination and exposure combinations on 4 datasets are shown in Fig. 5a and 5b. The experiment results show that the proposed algorithm performs relatively well in both cases compared to other test algorithms.

4.3 Results of Only Similarity Measure

In order to evaluate the results of only the proposed similarity measure, we used the Winner-Takes-All approach directly on the matching cost obtained. In this subsection we compared the proposed method with MC-CNN [16], which is an outstanding deep learning based matching cost algorithm for radiometric changes. Fig. 6 shows experiment results of each test matching cost using WTA on test data ‘Cloth4’ and ‘Rocks1’ with radiometric changes as subscripts shows. Experiment results show that the matching cost of proposed algorithm performed better than MC-CNN in some cases.

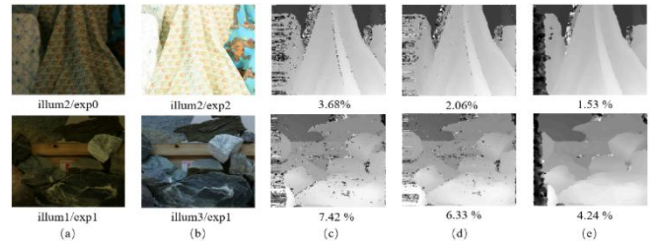


Figure 6. Disparity map obtained by test algorithms with WTA. (a) Left image. (b) Right image. (c) MC-CNN-fst. (d) MC-CNN-acrt. (e) The proposed algorithm.

4.4 Noise Variations

In order to test the robustness of the proposed matching cost algorithm on noisy images, we chose Gaussian noise for our experiment and added Gaussian noise to both the left and right image of ‘Dolls’ data set. In the noise-robustness experiment, we set four kinds of noise. Noise0: Without Gaussian noise; Noise1: Gaussian noise with variance of 10^{-3} (47.16db); Noise2: Gaussian noise with variance of 10^{-2} (27.17db); Noise3: Gaussian noise with variance of $2 * 10^{-2}$ (21.14db). Here, db is the unit of signal-to-noise-ratio(SNR).

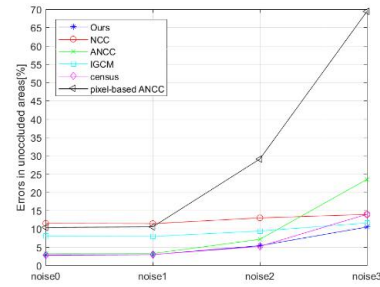


Figure 7. The average percentages of errors in unoccluded areas of test algorithms on noisy dolls data sets.

Fig. 7 shows the average percentages of errors in unoccluded areas of test algorithms on noisy dolls data sets. The blue curve indicates that proposed algorithm is relatively robust to noise variations. The proposed algorithm is more robust to noise, because it is mainly basing on gray-scale channel other than log-chromaticity color channel. And the proposed algorithm is window-based which can collect more information of pixels that are less affected than pixel-based algorithm.

5. CONCLUSION

Present matching cost algorithm suffer from non-robustness to image pairs with exposure changes, illumination changes and noise. To overcome this disadvantage, we propose a new matching cost algorithm, where an improved ZNCC model is presented to evaluate the similarity of the intensity between windows and a window-based LBP model to evaluate the similarity of the texture between windows. The proposed algorithm has a robust performance to radiometric changes and noisy image pairs. The proposed matching cost algorithm can be used with other cost aggregation algorithms, or as the initial matching cost of the global algorithm. Since the proposed algorithm is based on the windows to calculate the similarity of pixels, the algorithm is not as fast as the pixel-based algorithm.

6. ACKNOWLEDGMENT

This work is supported by the National Natural Science Foundation of China under Grant No. 61473330.

7. REFERENCES

- [1] Celebi M E, Smolka B. Advances in Low-Level Color Image Processing[M]. 2014.
- [2] H. Hirschmüller and D. Scharstein. Evaluation of cost functions for stereo matching. In IEEE Computer Society Conference on Computer Vision and Pattern Recognition(CVPR 2007), Minneapolis, MN, June 2007.
- [3] Hirschmüller H, Scharstein D. Evaluation of stereo matching costs on images with radiometric differences[J]. IEEE transactions on pattern analysis and machine intelligence, 2008, 31(9): 1582-1599.
- [4] Faugeras O, Hotz B, Mathieu H, et al. Real time correlation-based stereo: algorithm, implementations and applications[R]. Inria, 1993.
- [5] Zabih R . Non-parametric Local Transforms for Computing Visual Correspondence[J]. Computer Vision-ECCV '94, 1994.
- [6] Chrastek R, Jan J. Mutual information as a matching criterion for stereo pairs of images[J]. Analysis of Biomedical Signals and Images, 1998, 14(101-103): 22.
- [7] Kim J, Kolmogorov V, Zabih R. Visual correspondence using energy minimization and mutual information[C]//null. IEEE, 2003: 1033.
- [8] Hirschmüller H. Stereo processing by semi-global matching and mutual information[J]. IEEE Transactions on pattern analysis and machine intelligence, 2007, 30(2): 328-341.
- [9] Heo Y S, Lee K M, Lee S U. Robust stereo matching using adaptive normalized cross-correlation[J]. IEEE Transactions on Pattern Analysis and Machine Intelligence, 2010, 33(4): 807-822.
- [10] Khan A, Khan M U K, Kyung C M. Intensity guided cost metric for fast stereo matching under radiometric variations[J]. Optics Express, 2018, 26(4):4096.
- [11] Xu J, Yang, Qingxiong, Tang, Jinhui, et al. Linear Time Illumination Invariant Stereo Matching[J]. International Journal of Computer Vision, 2016, 119(2):179-193.
- [12] He K, Sun J, Tang X. Guided image filtering[J]. IEEE transactions on pattern analysis and machine intelligence, 2012, 35(6): 1397-1409.
- [13] Ojala T, Pietikainen M, Harwood D. A comparative study of texture measures with classification based on featured distributions[J]. Pattern recognition, 1996, 29(1): 51-59.
- [14] Chang Y J , Ho Y S . Pixel-Based Adaptive Normalized Cross Correlation for Illumination Invariant Stereo Matching[J]. Electronic Imaging, 2017, 2017(5):124-129.
- [15] Yang Q. A non-local cost aggregation method for stereo matching[C]//Computer Vision & Pattern Recognition. 2012.
- [16] Zbontar, Jure, Lecun Y . Stereo Matching by Training a Convolutional Neural Network to Compare Image Patches[J]. 2015.